Strain	Genotype	Source
PTY1053	*Mat a hht2,hhf2::natMX4*, *hht1,hhf1::kanMX4* pURA3-*HTA1-HTB1*	(Tessarz and Kouzarides, 2014)
HSR362	*Mat a hht2,hhf2::natMX4*, *hht1,hhf1::kanMX4* *TRP1-HHT2-HHF2*	(Tessarz and Kouzarides, 2014)
HSR364	*Mat a hht2,hhf2::natMX4*, *hht1,hhf1::kanMX4* *TRP1-HHT2 K37A-HHF2*	This study
HSR436	*Mat a hht2,hhf2::natMX4*, *hht1,hhf1::kanMX4* *TRP1-HHT2K37R-HHF2*	This study
HSR660	*Mat a hht2,hhf2::natMX4*, *hht1,hhf1::kanMX4* *TRP1-HHT2K36R-HHF2*	This study
HSR662	*Mat a hht2,hhf2::natMX4*, *hht1,hhf1::kanMX4* *TRP1-HHT2K4R-HHF2*	This study
HSR688	*Mat a hht2,hhf2::natMX4*, *hht1,hhf1::kanMX4* *TRP1-HHT2K4R-HHF2 set2::HIS3*	This study
HSR691	*Mat a hht2,hhf2::natMX4*, *hht1,hhf1::kanMX4* *TRP1-HHT2K36R-HHF2 set1::3ARU*	This study
HSR416	*Mat a hht2,hhf2::natMX4*, *hht1,hhf1::kanMX4* *TRP1-HHT2-HHF2 MCM2-HA_6::HYGRO*	This study
HSR453	*Mat a hht2,hhf2::natMX4*, *hht1,hhf1::kanMX4* *TRP1-HHT2-HHF2 HIS3*::*GPD–TK_7*	This study

HSR454	*Mat a hht2,hhf2::natMX4, hht1,hhf1::kanMX4 TRP1-HHT2K37R-HHF2 HIS3::GPD–TK7*	This study
HSR438	*Mat a hht2,hhf2::natMX4, hht1,hhf1::kanMX4 TRP1-HHT2K37R-HHF2 MCM2-HA6::HYGRO*	This study
HSR707	*Mat a hht2,hhf2::natMX4, hht1,hhf1::kanMX4 TRP1-HHT2-HHF2 CDC45-HA6::HYGRO*	This study
HSR708	*Mat a hht2,hhf2::natMX4, hht1,hhf1::kanMX4 TRP1-HHT2K37R-HHF2 CDC45-HA6::HYGRO*	This study
W303	*Mat a ade2-1 can1-100 his3-11,15 leu2-3,112 trp1-1 ura3-1*	Rodney Rothstein
HSR645	*Mat a ade2-1 can1-100 his3-11,15 leu2-3,112 trp1-1 ura3-1 set1::3ARU*	This study
HSR643	*Mat a ade2-1 can1-100 his3-11,15 leu2-3,112 trp1-1 ura3-1 set2::HIS3*	This study
HSR646	*Mat a ade2-1 can1-100 his3-11,15 leu2-3,112 trp1-1ura31 set1::3ARU set2::HIS3*	This study
HSR495 (7Δ)	*Mat a ade2-1 can1-100 his3-11,15 leu2-3,112 trp1-1 ura31 set1N1016Q::LEU2 set2::HIS3 set3::NAT set4::KAN MX set5::TRP1 set6::URA3 set7::ADE2*	This study
HSR727	*Mat a hht2,hhf2::natMX4, hht1,hhf1::kanMX4 LEU2- Gal1-10 CDC45/SLD7 TRP1- Gal1-10 SLD2/DPB11 URA3-Gal1-10 SLD3/DBF4 ADE2-HHT2-HHF2 HIS3::GPD–TK7*	This study
HSR729	*Mat a hht2,hhf2::natMX4, hht1,hhf1::kanMX4 LEU2- Gal1-10 CDC45/SLD7 TRP1- Gal1-10 SLD2/DPB11*	This study

	URA3-Gal1-10 SLD3/DBF4 ADE2-HHT2K37R-HHF2 HIS3::*GPD–TK*$_7$	
SK1	*Mat* a/α *HO gal2 cup*^{S} *can1*^{R} *BIO*	(Kane and Roth, 1974)
ID 15459	*h90 ade6-216 leu1-32 lys1-131 ura4-d18 mcm3::MCM3-GFP-HÁ-KAN MX*	NRBP (http://yeast.nig.ac.jp/yeast/)

Table S1. Yeast Strains used in this study. Strains are derivatives of W303. Histone point mutants were shuffled into yeast by counter-selection on 5-FOA. The screen for the H3 K37me1 enzymes was performed using the Euroscarf BY4743 wild type and curate isogenic deletion strain collection (Puddu et al., 2019). Methyltransferases not properly disrupted or missing from the collection were deleted in BY4141 for this study and compared to the isogenic WT.

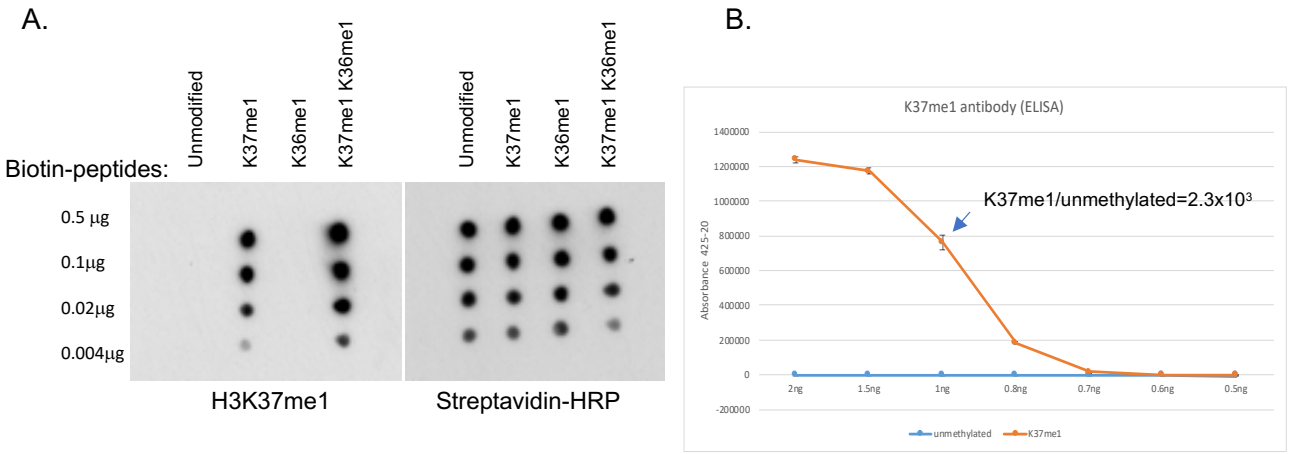

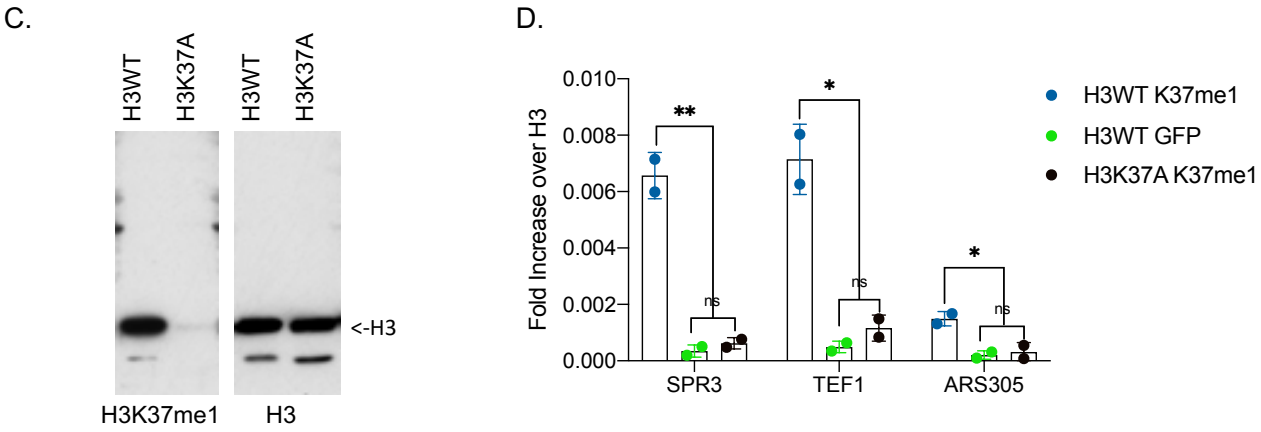

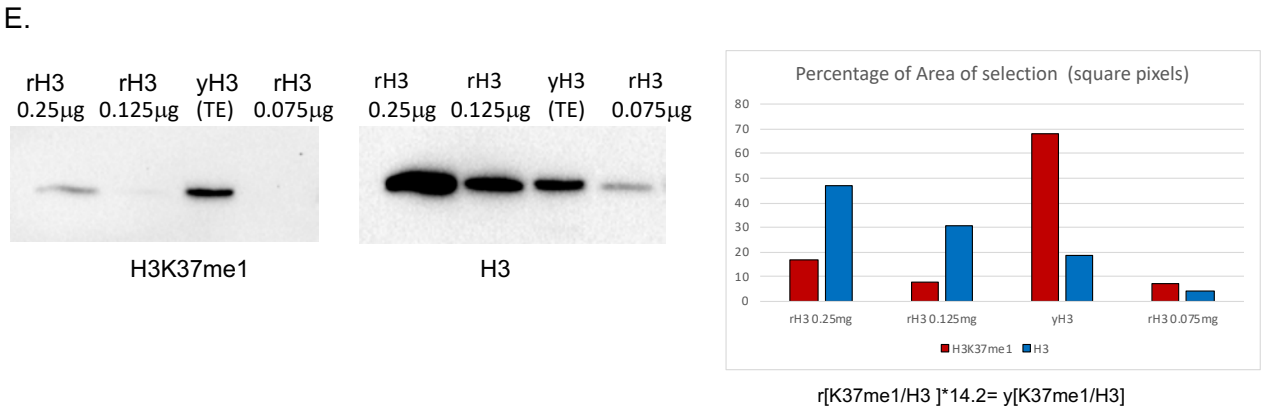

r[K37me1/H3]*14.2= y[K37me1/H3]

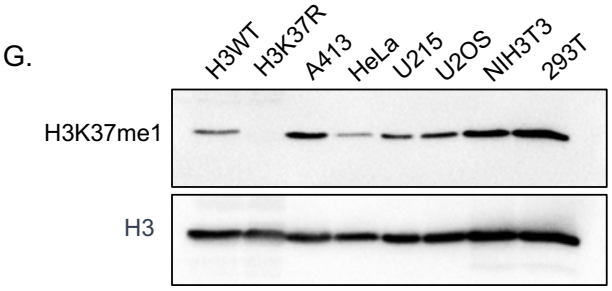

Supplementary Figure 1

Figure S1. Characterization of H3K37me1 monoclonal antibody. Related to Figure 1. Dot-blot analysis using H3K37me1 specific antibody. 5-fold serial dilutions of different biotinylated H3 peptides (aa28-aa48), as indicated, were spotted onto a PVDF membrane. The membrane was subsequently blotted with Streptavidin-HRP for a loading control. **(B)** Direct enzyme-linked immunosorbent assay (ELISA) against the indicated peptides. **(C)** Immunoblot analysis of purified yeast histones. H3WT and isogenic H3K37A mutant cells were grown to exponential phase. Purified yeast histones were separated by SDS-PAGE in 16% acrylamide gels. Blots were probed with anti-H3K37me1 antibody and then re-probed with an anti-H3 antibody as indicated. **(D)** ChIP qPCR experiments showing H3K37me1 levels at different genomic locations. H3WT and H3K37A strains were crosslinked and chromatin was immunoprecipitated (IP) using anti-H3K37me1, anti-H3 or anti-GFP antibodies. Statistical analysis was performed using multiple t test corrected for the comparisons using the Holm-Sidak method (Alpha: 0.05); * - $P \leq 0.05$, ** - $P \leq 0.01$. Error bars represent the mean ± SD of 2 independent experiments. **(E)** Immunoblot analysis of unmodified recombinant H3 (rH3) *versus* yeast total extracts (yH3, TE). Blots were probed with anti-H3K37me1 antibody and then re-probed with anti-H3 antibody as indicated. **(F)** Quantification of immunoblots shown in (E). **(G)** Immunoblot analysis of total protein extracts from different mammalian cell lines as indicated. Proteins were separated by SDS-PAGE in 16% acrylamide gels. Blots were probed with anti-H3K37me1 antibody and then re-probed with anti-H3 antibody as indicated. Wild-type H3 and H3K37R mutant were used as controls.

A.

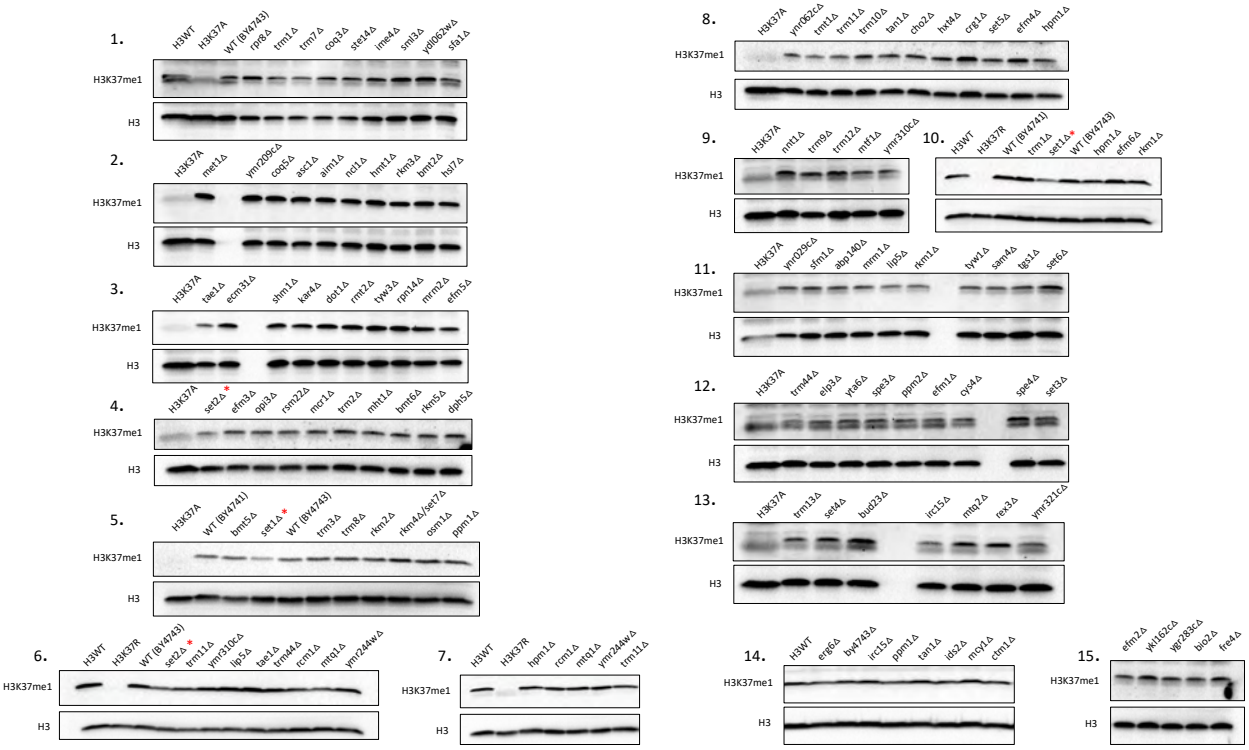

B.

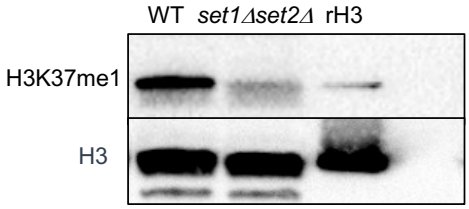

C.

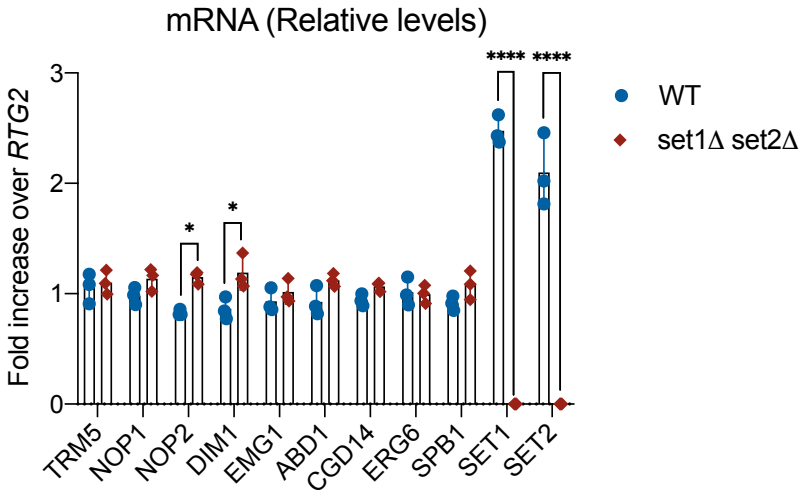

Supplementary Figure 2

Figure S2. Set1 (COMPASS) and Set2 are responsible for H3 K37me1 *in vivo*. Related to Figure 1. (A) Immunoblot analysis of total protein extracts from wild-types (BY4741 and BY4743) and isogenic deletion mutants as specified. Proteins were separated by SDS-PAGE in 16% acrylamide gels. Blots were probed with anti-H3K37me1 antibody and then re-probed with anti-H3 antibody as indicated. H3WT and isogenic H3K37A/R mutants were used as controls. *set1Δ* and *set2Δ* are highlighted *. **(B)** Immunoblot analysis of unmodified recombinant H3 (rH3) *versus* yeast wild-type and *set1Δset2Δ* total extracts. Blots were probed with anti-H3K37me1 antibody and then re-probed with anti-H3 antibody as indicated.

(C) RT-PCR showing mRNA levels of essential methyltransferases in wild-type (W303) and *set1Δset2Δ* isogenic strain. The housekeeping transcript *RTG2* was used for internal normalization. Statistical analysis was performed using multiple t -test corrected for the comparisons using the Holm-Sidak method (Alpha: 0.05); * - $P \leq 0.05$, ** - $P \leq 0.01$. Error bars represent the mean ± SD of 3 biological replicates.

A.

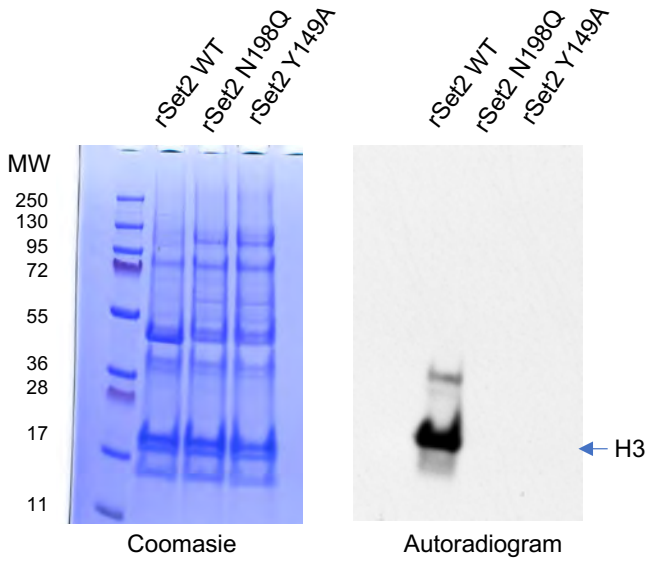

B.

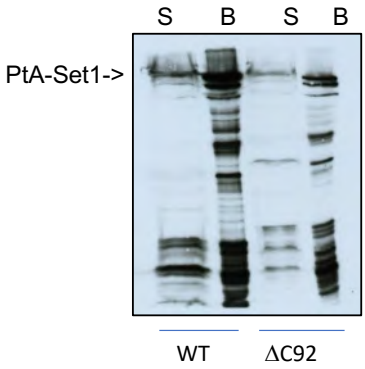

PtA-Set1 Purification

C.

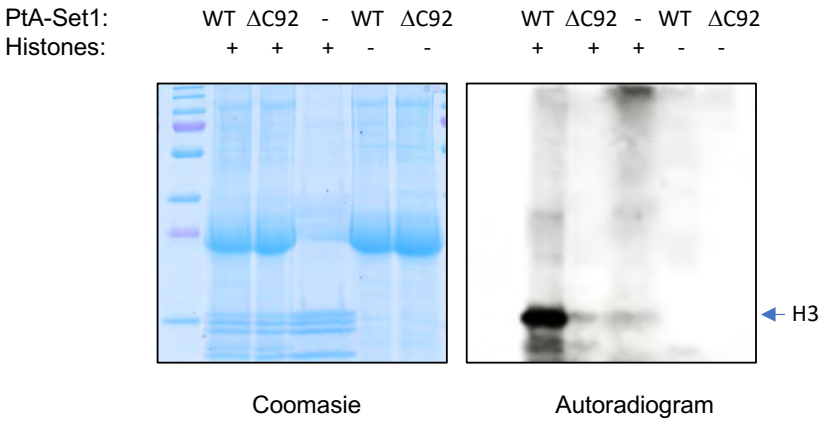

Supplementary Figure 3

Figure S3. Set1 (COMPASS) and Set2 *in vitro* activity. Related to Figure 2. (A) ^{3}H-SAM dependent methyltransferase reactions on calf thymus histones, catalysed by recombinant wild-type (WT) Set2p, Set2N198Qp and Set2Y149Ap. Reactions were separated in a NuPAGE 4-12% gel. Left panel: Coomasie Blue staining. Right panel: Autoradiogram. H3 is highlighted. **(B)** IgG chromatography purification of WT PtA-Set1p and PtA-set1ΔC92p. Complexes were resolved by SDS-PAGE in 16% acrylamide gels. Set1p and set1ΔC92p were detected by immunoblot using anti-PAP antibody. S: yeast soluble input, B: beads bound fraction. **(C)** ^{3}H-SAM dependent methyltransferase reactions on calf thymus histones, catalysed by equal amounts of wild-type PtA-Set1p and PtA-set1ΔC92p yeast purified complexes. Reactions were separated in NuPAGE 4-12% gel. Left panel: Coomasie Blue staining. Right panel: Autoradiogram. H3 is highlighted.

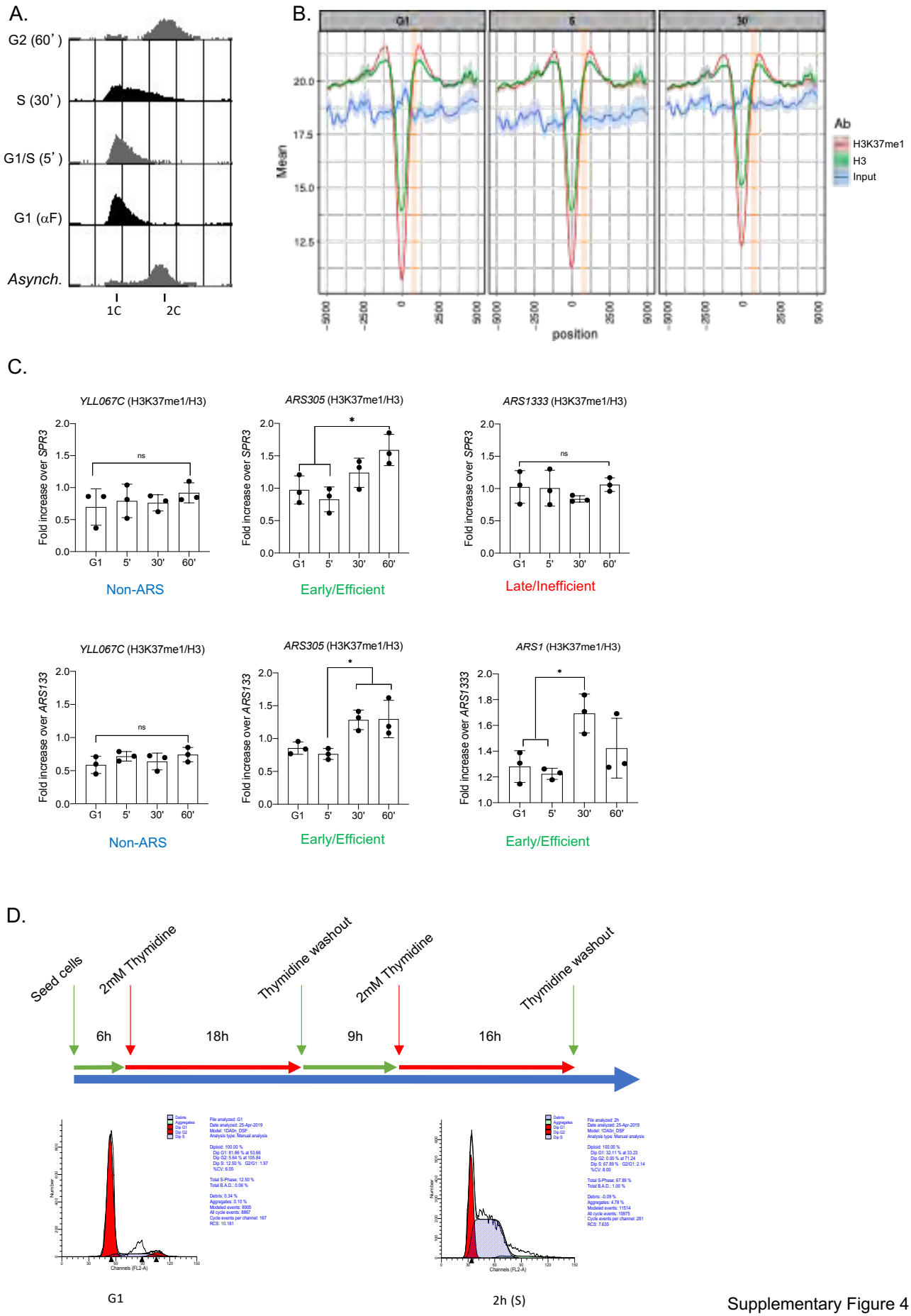

Supplementary Figure 4

Figure S4. H3 K37me1 is cell cycle regulated at replication origins. Related to Figure 3. (A) Flow cytometry analysis. Wild-type cells were arrested in G1 using α-factor, released into the cell cycle and samples were collected at the specified times. **(B)** Coverage plot showing the mean normalised ChIP-signal (+/- s.e.m.) for H3, H3K37me1 and Input at Transcription Start Sites +/-5kb. The time points (G1, 5' and 30') correspond to those in Fig.3B. **(C)** ChIP qPCR experiments showing H3K37me1 levels at different genomic locations. Wild-type cells were arrested in G1using α-factor and released into the cell cycle. Chromatin from G1, 5' 30' and 60' time points was immunoprecipitated using anti-H3K37me1 and anti-H3 antibodies. H3K37me1 enrichment over H3 was normalized to a non-*ARS* region (*SPR3*) and to a late/inefficient *ARS* (*ARS1333*). Statistical analysis was performed using One-way ANOVA multiple comparisons using Tukey's multiple comparison test (Alpha: 0.05); * - $P \leq 0.05$, ** - $P \leq 0.01$. Error bars represent the mean ± SD of 3 independent experiments. **(D)** Experimental design for double thymidine arrest and flow cytometry analysis of RPE1 cell cultures used for G1->S H3K37me1 chromatin immunoprecipitation experiments shown in Figure 3F.

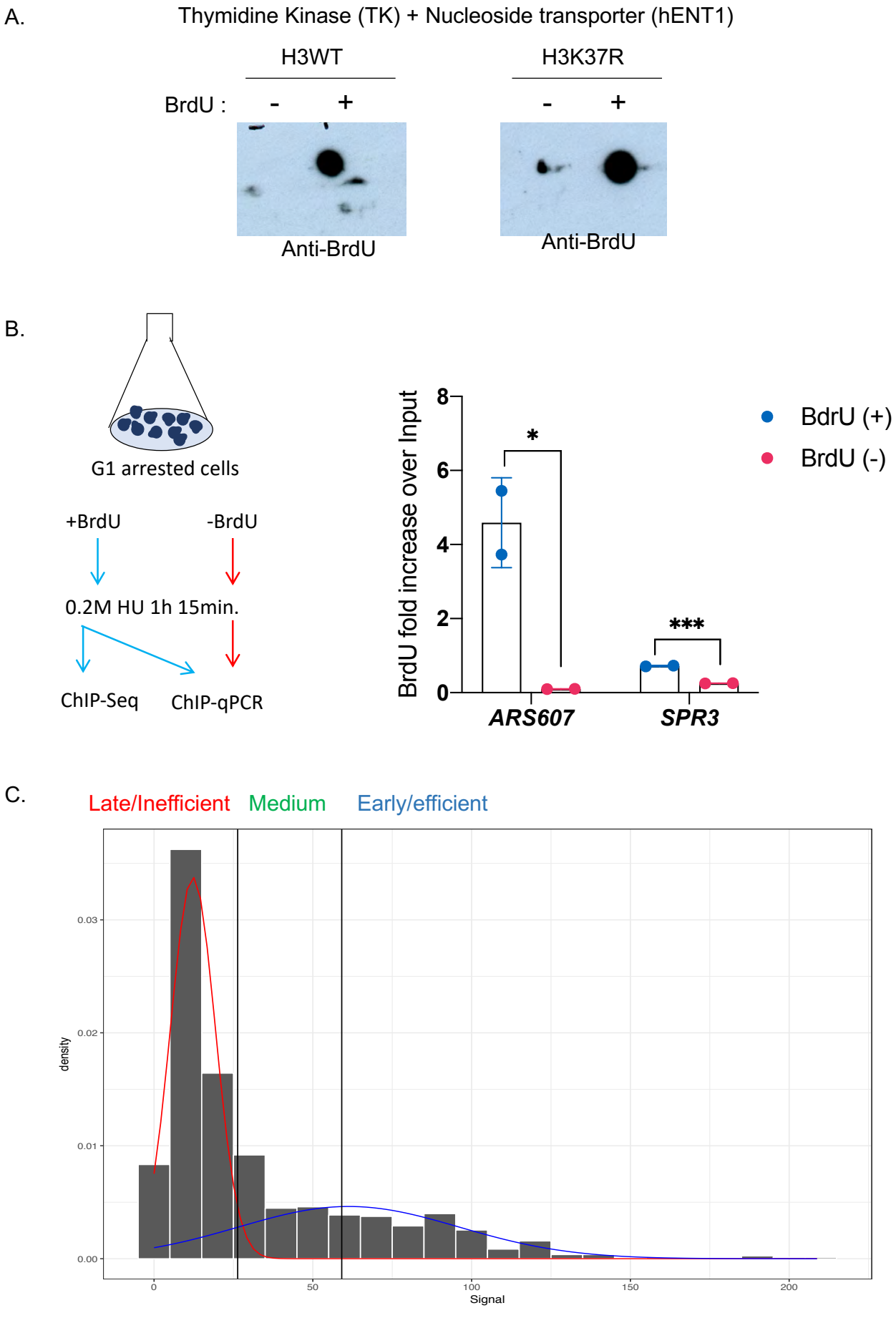

Supplementary Figure 5

Figure S5. DNA replication profiling of H3WT and H3K37R mutant. Related to Figure 4. (A) BrdU incorporation of H3WT and isogenic H3K37R mutant strains. Equal amounts of DNA from H3WT and H3K37R cells incubated in the absence (-) or presence (+) of BrdU was immunoblotted with anti-BrdU antibody. **(B) Left:** Experimental design for DNA replication profiling experiments. **Right:** Equal amounts of DNA from H3WT cells incubated in the absence (-) or presence (+) of BrdU was immunoprecipitated using anti-BrdU antibody. IP material was quantified by qPCR using specific primers as indicated. Statistical analysis was performed using multiple t-test corrected for the comparisons using the Holm-Sidak method (Alpha: 0.05); * - $P \leq 0.05$, ** - $P \leq 0.01$. Error bars represent the mean ± SD of 2 independent experiments. **(C)** Distribution of BrdU IP signal intensity at replication origins. y-axis shows the probability densities, indicating the frequencies of ARSs observed at different BrdU intensity levels (x-axis: Signal), as estimated by the kernel density function. Red and Blue lines represent the components of a Gaussian Mixture Model corresponding, respectively, to non-active and active *ARS* in a H3 wild-type strain under the experimental conditions described in (B).

A.

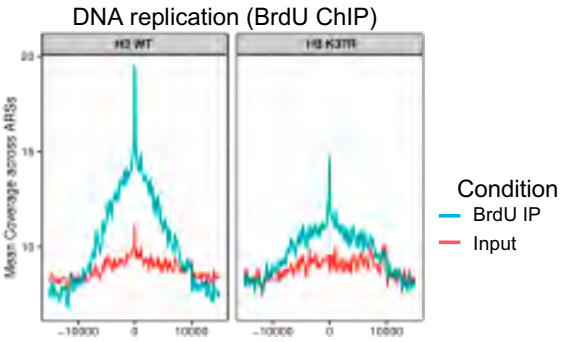

B.

C.

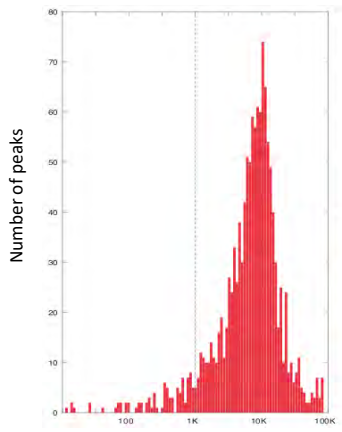

D.

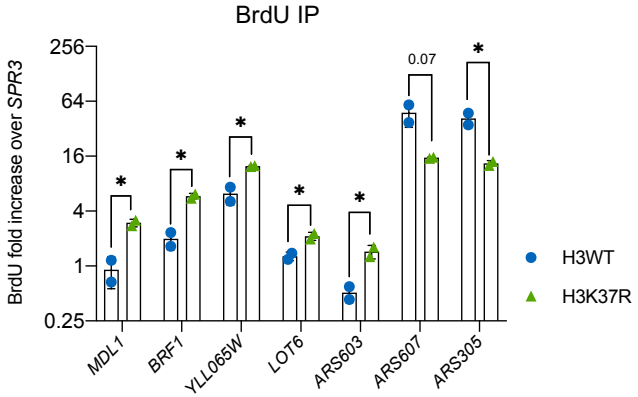

Supplementary Figure 6

Figure S6. Lack of H3K37me1 results in genome-wide spurious replication events. Related to Figure 4. (A) Coverage plot of the mean signal across all *ARS* shown in (Fig.4A) centred at *ACS* (Ars Consensus Sequence). Input (red); IP (blue). **(B)** Representative genome browser snapshots of BrdU incorporation in H3WT and isogenic H3K37R mutant cells at different chromosomal locations. H3K37R statistically significant unique peaks are highlighted (green). Locations chosen for further analysis are labelled by green boxes. The plots represent the average of 4 independent experiments. **(C)** Distribution of H3K37R unique peaks relative to the nearest confirmed *ARS*. Note the logarithmic scale on *x-axis*. **(D)** BrdU incorporation in H3WT and H3K37R mutant cells analysed by qPCRs at different genomic locations with specific primers. The data correspond to the experiment shown in Fig.4D but normalized to a non-*ARS* region (*SPR3*) instead to "IP fold increase over Input". Error bars represent the mean ± SD of 2 biological replicates. Statistical analysis was performed using multiple t test without correction for multiple comparisons (Alpha: 0.05); * - $P \leq 0.05$, ** - $P \leq 0.01$, *** - $P \leq 0.001$, **** - $P \leq 0.0001$. Note the logarithmic scale on *y-axis*.

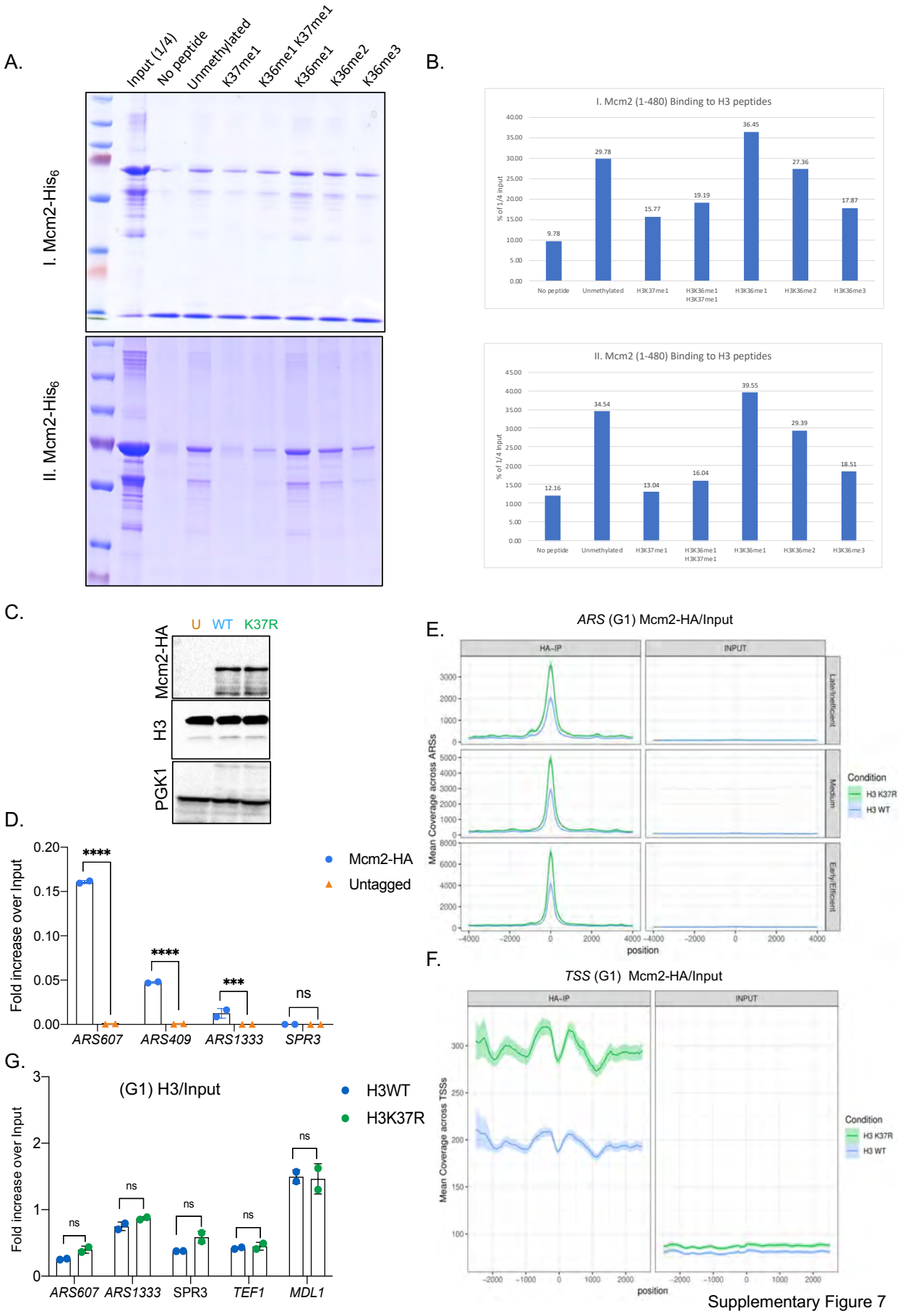

Supplementary Figure 7

Figure S7. Lack of H3K37me1 results in genome-wide increased MCM recruitment to chromatin. Related to Figure 5. (A) Mcm2-His_6 *in vitro* binding to biotinylated H3 peptides, modified as indicated. Input and peptide-bound Mcm2 were resolved by SDS-PAGE in 10% (assay I) or 8% (assay II) acrylamide gels and detected by Coomasie-Brilliant Blue (CBB) staining. I. (shown in Fig.5A) and II are independent binding assays. **(B)** Quantification of assays I and II Coomasie binding signal by ImageJ. Binding is represented as % of the signal corresponding to ¼ of the input. **(C)** Immunoblot analysis of total protein extract from G1-arrested untagged and Mcm2-HA tagged cells. Proteins were separated by SDS-PAGE in either 8% gels for Mcm2-HA or 16% acrylamide gels for H3 detection. Blots were probed with anti-HA or anti-H3 antibodies and then re-probed with an anti-PGK1 antibody as loading control. U: untagged-Mcm2 H3WT, WT: Mcm2-HA H3WT, K37R: Mcm2-HA H3K37R. **(D)** ChIP qPCR experiments showing MCM2-HA levels at different locations. H3WT expressing Mcm2-HA (blue) or untagged Mcm2 (orange) cells were crosslinked and chromatin was immunoprecipitated (IP) with anti-HA antibody. IPs were analysed by qPCRs at different genomic locations with specific primers. Statistical analysis was performed using Two-way ANOVA corrected for the comparisons using the Holm-Sidak method (Alpha: 0.05); * - $P \leq 0.05$, ** - $P \leq 0.01$, *** - $P \leq 0.001$, **** - $P \leq 0.0001$. Error bars represent the mean ± SD of 2 independent experiments **(E)** Coverage plots of Mcm2-HA occupancy at early/efficient, medium and late/inefficient *ARS*s centred at *ACS* (Ars Consensus Sequence) **Left:** G1 Mcm2-HA IP. **Right:** G1 Input. **(F)** Coverage plots of Mcm2- HA occupancy at non-*ARS* regions centred at *TSS* (Transcription Start Sites). **Left:** G1 Mcm2-HA IP. **Right:** G1 Input. Data correspond to the average of 3 independent cultures for each strain. Note the difference in the scale between (E) and (F). **(G)** ChIP qPCR experiments showing H3 levels at different locations. H3WT and H3K37R yeast cells expressing Mcm2-HA were arrested in G1, crosslinked and chromatin was immunoprecipitated (IP) with anti-H3 antibody. The IP material was analyzed by qPCR with primers specific for each location. Statistical analysis was performed using Two-way ANOVA corrected for the comparisons using the Holm-Sidak method. "ns" refers to non-statistical significance. Error bars represent the mean ± SD of 2 biological replicates.

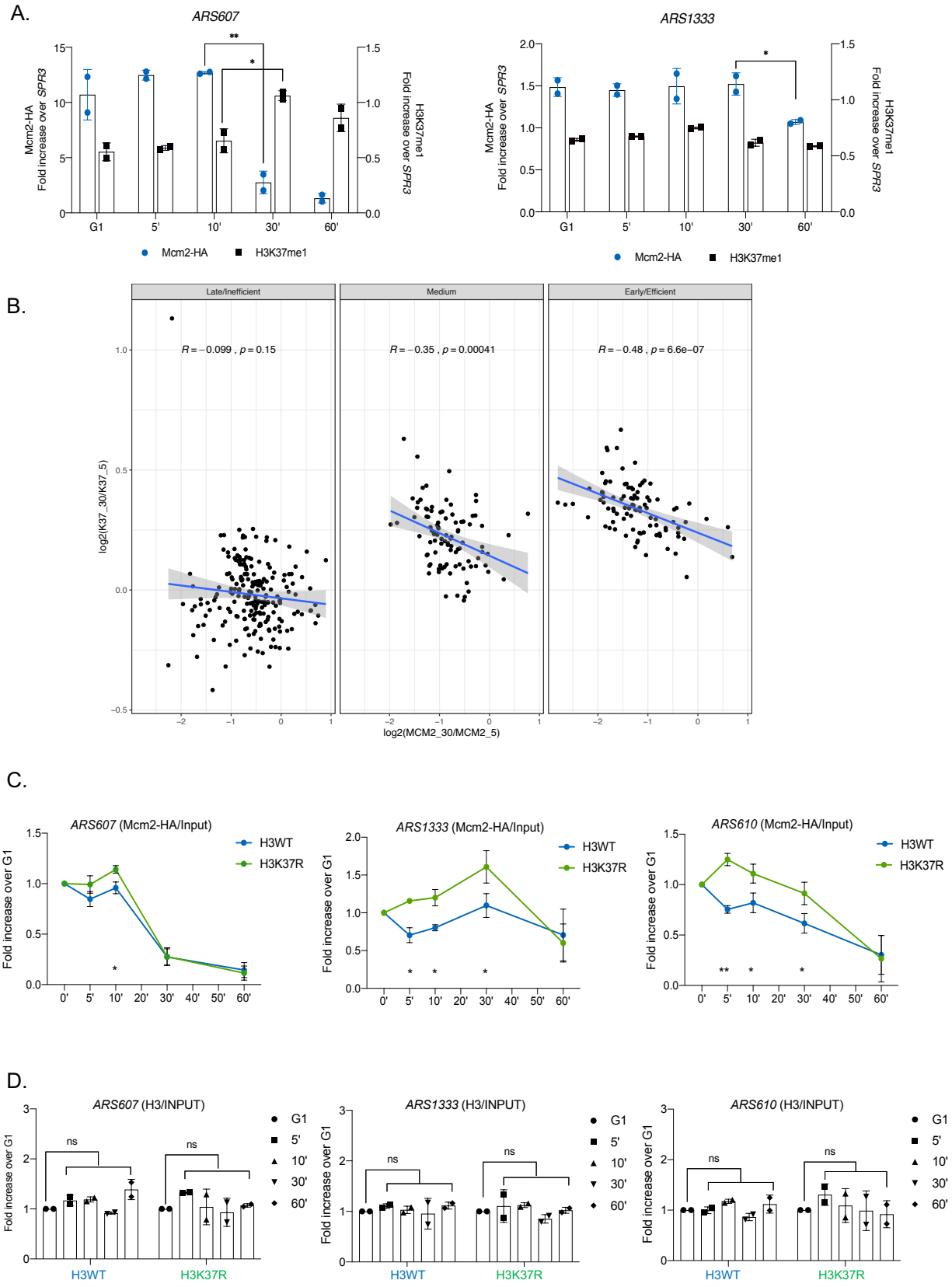

Supplementary Figure 8

Figure S8. H3K37me1 and MCM anticorrelate on chromatin during the cell cycle. Related to Figure 5. (A) Time course ChIP qPCR experiments showing Mcm2-HA and H3K37me1 levels at *ARSs*. Wild-type cells were arrested in G1, released into the cycle and chromatin samples from indicated times were immunoprecipitated using anti-HA, anti-H3K37me1 and anti-H3 antibodies. The IP material was analyzed by qPCR with primers towards efficient *ARS607* or inefficient *ARS1333* and normalized to a non-*ARS* region (*SPR3*). Statistical analysis was performed using multiple t test without correction for multiple comparisons (Alpha: 0.05); * - $P \leq 0.05$, ** - $P \leq 0.01$. Error bars represent the mean ± SD of 2 independent experiments. **(B)** Scatter plot (log_2 30'/5' released from G1) representing Mcm2 (*x-axis*) *versus* H3K37me1 (*y-axis*) at early/efficient, medium and late/inefficient *ARS*s. **(C)** ChIP qPCR experiments showing Mcm2-HA during a time course in wild-type and H3K37R mutant. Cells were arrested in G1, released into the cycle and chromatin samples from indicated times was immunoprecipitated using anti-HA antibody. The IP material was analyzed by qPCR with primers specific towards late/inefficient (*ARS1333* and *ARS610*) and early/efficient (*ARS607*) replication origins. Time points are normalized to the G1 signal. Statistical analysis was performed using multiple t test without correction for multiple comparisons (Alpha: 0.05); * - $P \leq 0.05$, ** - $P \leq 0.01$. Error bars represent the mean ± SD of 2 independent experiments. **(D)** ChIP qPCR experiments showing H3 levels during the time course shown in (C). The IP material was analyzed by qPCR with primers specific towards late/inefficient (*ARS1333* and *ARS610*) and early/efficient (*ARS607*) replication origins. Time points are normalized to the G1 signal. Statistical analysis was performed using multiple t test without correction for multiple comparisons. "ns" refers to non-statistical significance. Error bars represent the mean ± SD of 2 independent experiments.

A.

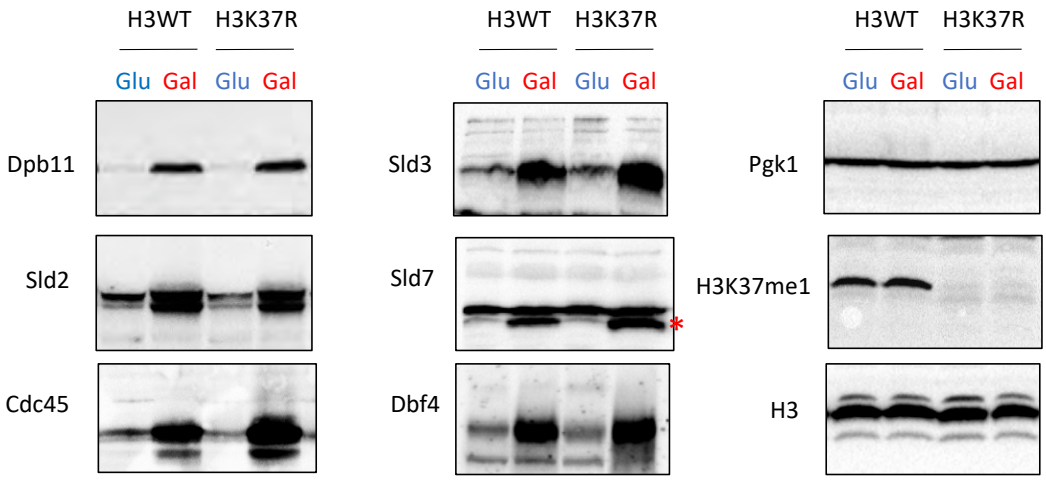

B.

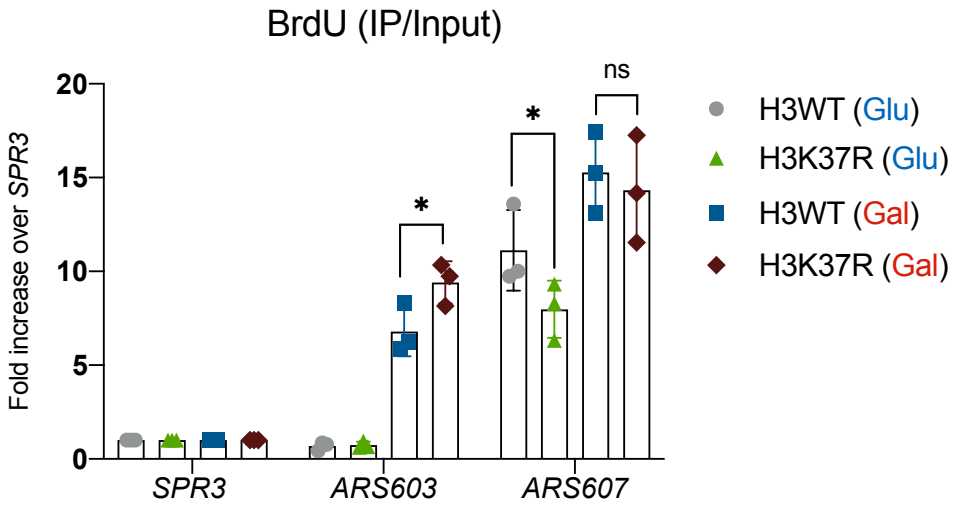

C.

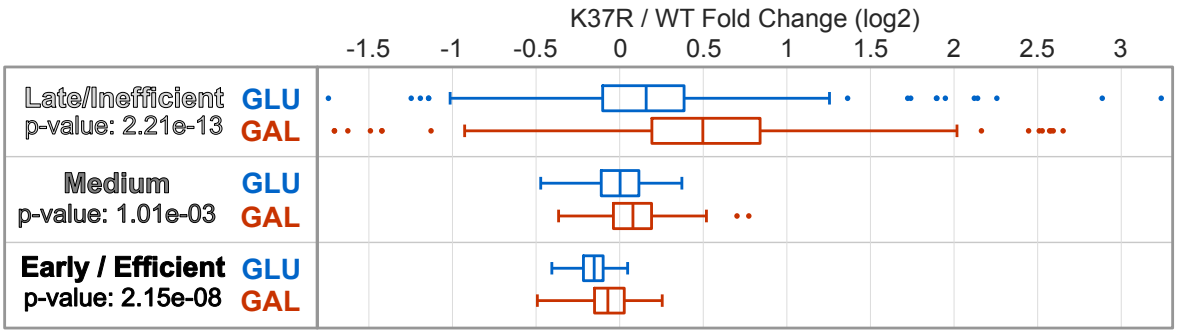

Supplementary Figure 9

Figure S9. Overexpression of the MCM activators suppresses the H3H37R replication defect. **Related to Figure 6. (A)** Immunoblot analysis of total H3WT and isogenic H3K37R mutant extracts prepared under "non-induced" (Glucose) and "induced overexpression" (Galactose) of the MCM helicase activators as described in M&M. Blots were probed with antibodies specific to each of the activators (generous gift from H. Araki) and anti-H3K37me1 antibodies as indicated. Anti-Pgk1 and anti-H3 were used as controls. Sld7 specific signal is highlighted *. **(B)** BrdU incorporation in H3WT and isogenic H3K37R mutant strains. Equal amounts of DNA from H3WT and H3K37R cells grown in the presence of BrdU under "non-induced" (Glucose) and "induced overexpression" (Galactose) of the MCM helicase activators, were immunoprecipitated using anti-BrdU antibody. IP material was quantified by qPCR using primers specific towards late/inefficient *ARS603 or* early/efficient *ARS607*, then normalized to a non-*ARS* region (*SPR3*). Statistical analysis was performed using multiple t test without correction for multiple comparisons (Alpha: 0.05); * - $P \leq 0.05$, ** - $P \leq 0.01$. Error bars represent the mean ± SD of 3 independent colonies. **(C)** Box-plot showing the distribution of mean BrdU signal (H3K37R/H3WT ratio) incorporated at the replication origins shown in B. The p-values were calculated with the Mann-Whitney-Wilcoxon test.

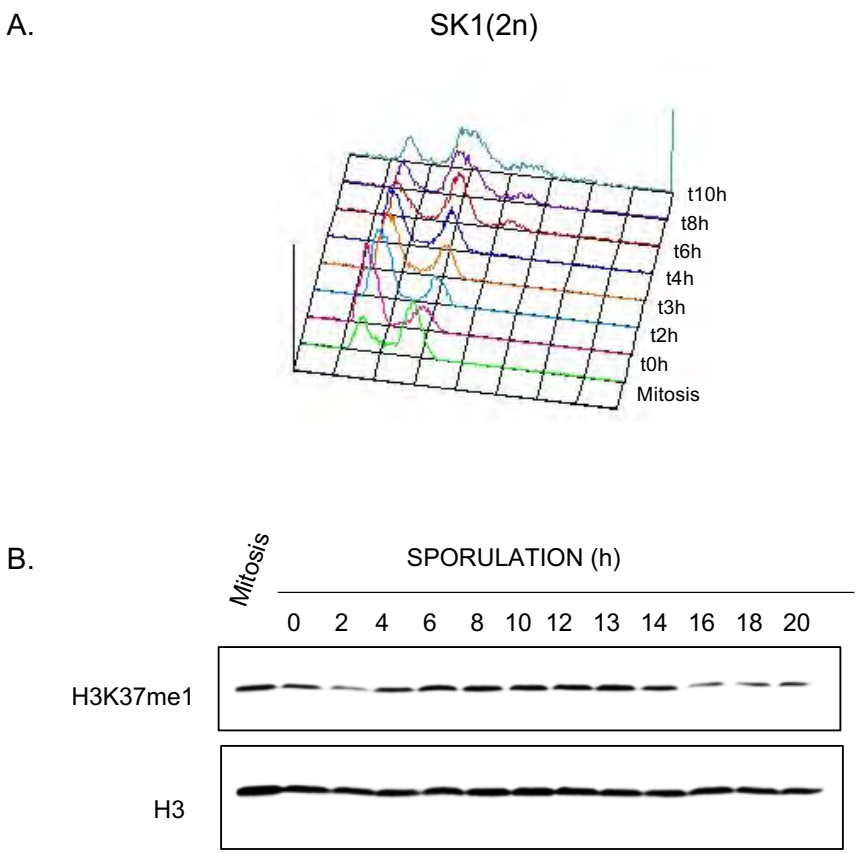

Supplementary Figure 10

Figure S10. H3 K37me1 increases during premeiotic DNA replication. Related to Discussion. SK1 diploid cells were G1 enriched by nutrient starvation and released to sporulation medium. Samples for FACS and protein total extracts were collected at the specified times. **(A)** Flow cytometry analysis. **(B)** Proteins were separated by SDS-PAGE in 16% acrylamide gels and probed with anti-H3K37me1 antibody and then re-probed with an anti-H3 antibody as indicated.